

# Solvent-sensitive charge-transfer absorption behaviours and dual-emissive fluorescent properties of a thiazole-conjugated pyridinium complex†

Zhan-Xian Li,<sup>ab</sup> Chun-Hu Xu,<sup>a</sup> Wei Sun,<sup>a</sup> Yan-Chun Bai,<sup>a</sup> Chao Zhang,<sup>a</sup>  
Chen-Jie Fang<sup>a</sup> and Chun-Hua Yan<sup>\*a</sup>

Received (in Montpellier, France) 27th October 2008, Accepted 17th December 2008

First published as an Advance Article on the web 28th January 2009

DOI: 10.1039/b819016j

A new fluorophore, 1-(ethoxy-carbonyl-methyl)-4-[2-(5-methoxy)thiazolyl]pyridinium bromide (**4-MeB**), has been synthesized and its photophysical properties investigated. In solvents with a larger dielectric constant ( $\epsilon$ ), **4-MeB** is ionized into free ions, showing a characteristic thiazolyl-pyridinium cation-centered  $\pi \rightarrow \pi^*$  electronic transition absorption band in the UV region. In solvents with smaller  $\epsilon$  values, such as tetrahydrofuran (THF), 1,4-dioxane (dioxane) and ethyl acetate (EtOAc), **4-MeB** exists in the form of a tight ion pair, and concomitantly displays characteristic bromide anion-dependent absorption in the visible and UV regions. Among several other anions, such as  $\text{PF}_6^-$ ,  $\text{I}^-$  and  $\text{Cl}^-$ , and neutral electron donor  $\text{Et}_3\text{N}$ , only  $\text{I}^-$  shows a similar influence on the absorption spectrum of **4-Me**<sup>+</sup> to that of bromide anion, confirming the bromide-dependent spectral properties of **4-MeB**. With the help of theoretical calculations, the absorption in visible region is attributed to the charge-transfer from bromide anion to thiazolyl-pyridinium cation, which is tuned by the distance between the bromide anion and the thiazolyl-pyridyl moiety. In all of the solvents employed, **4-MeB** also exhibits a dual-emissive fluorescent property, and the position of its emission peak is influenced by the excitation wavelength.

## 1. Introduction

Since anions play important chemical and biological roles in many areas, such as in anion sensors,<sup>1–3</sup> self-assembly reactions,<sup>4–6</sup> photosynthesis<sup>7</sup> and luminescent materials,<sup>8</sup> the properties and mechanisms of non-covalent interactions involving anions have attracted much research interest in the field of supramolecular chemistry.<sup>1,9–11</sup> These non-covalent interactions mainly include hydrogen bonding,<sup>2,3,12–15</sup> coordination between anions and organometallic ligands or Lewis acids,<sup>4,12,16,17</sup> and anion– $\pi$  interactions.<sup>1,8,18</sup> Recently, we reported a highly luminescent fluorophore, *N*-[2-(1',3',4,4',5',5'-hexafluorocyclopentenyl)]-4-(5-methoxy-thiazolyl)pyridine (**4-MePF**), in which the interactions between the pyridinium  $\pi$  cation and allyl-type anion, conjugated through a covalent bond, contribute significantly to its spectral properties.<sup>19</sup> Until now, much of the work concerning anion– $\pi$  interactions has been focused on the effect of solvent on iodide anion– $\pi$  interactions,<sup>20–23</sup> with less studies on bromide anion– $\pi$  interactions.<sup>24</sup> Compared with iodine, bromine exhibits a larger electronegativity and a smaller anionic radius, which performs differently in anion– $\pi$  interactions.

Therefore, we are motivated to investigate the mechanism and influencing factors of intramolecular bromide anion– $\pi$  interactions. In the present work, we report the synthesis and photophysical properties of a new molecule, 1-(ethoxy-carbonyl-methyl)-4-[2-(5-methoxy)thiazolyl]pyridinium bromide (**4-MeB**), bearing a bromide anion. Investigations on the absorption spectrum of **4-MeB** in different solvents, combined with theoretical calculation results, reveal that its solvent-sensitive absorption properties originate from its different states in different solvents. In solvents with larger  $\epsilon$  values, **4-MeB** is ionized into free ions and shows the characteristic thiazolyl-pyridinium cation-centered  $\pi \rightarrow \pi^*$  electronic transition absorption in the UV region. However, in solvents with smaller  $\epsilon$  values, **4-MeB** exists in the form of a tight ion pair, and displays absorption bands in the visible and UV regions that originates from anion  $\rightarrow \pi$  charge-transfer. Studies on the fluorescence properties of **4-MeB** demonstrate that, in all the employed solvents, its dual-emissive property is influenced by the excitation wavelength.

## 2. Experimental section

### Chemicals and instruments

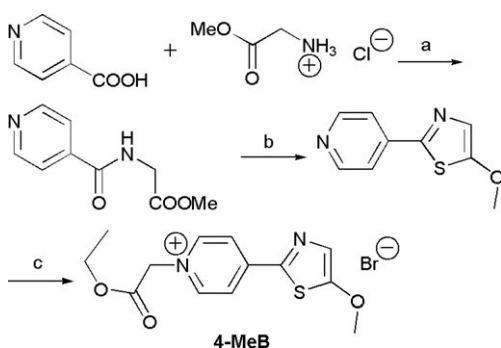
All chemicals were purchased from commercial suppliers and used without further purification. All reactions were performed under an argon atmosphere with solvents purified by standard methods.

<sup>1</sup>H and <sup>13</sup>C NMR spectra were recorded on a Bruker 400 spectrometer. Chemical shifts are reported in ppm using tetramethylsilane (TMS) as the internal standard. Mass spectra were obtained on an LCQ Deca XP Plus mass

<sup>a</sup> Beijing National Laboratory for Molecular Sciences, State Key Laboratory of Rare Earth Materials Chemistry and Applications, PKU-HKU Joint Laboratory in Rare Earth Materials and Bioinorganic Chemistry, Peking University, Beijing 100871, China. E-mail: yan@pku.edu.cn; Fax: +86 10-6275-4179

<sup>b</sup> Laboratory of Functional Materials, Department of Chemistry, Zhengzhou University, Zhengzhou 450001, China

† Electronic supplementary information (ESI) available: Absorption spectra, theoretical calculation results, fluorescence emission and excitation spectra, radiative decay curves, and fluorescence lifetimes of **4-MeB**. See DOI: 10.1039/b819016j



**Scheme 1** The synthetic route to compound **4-MeB**. a: Triethylamine, chloroform, 0 °C. b: Lawesson's reagent, toluene, reflux. c: Ethyl bromoacetate, chloroform, 20 °C.

spectrometer. Elemental analyses (C, H and N) were performed on an Elementary Vario EL analyzer. All spectral characterizations were carried out in HPLC grade solvents at 20 °C within a 10 mm quartz cell. UV-vis absorption spectra were measured using a Shimadzu UV-3100 spectrometer, and fluorescence spectra were determined on a Hitachi F-4500 spectrometer. Fluorescence lifetimes were obtained from an Edinburgh LifeSpec-ps fluorescence lifetime spectrometer. DFT calculations were carried out using GAUSSIAN 03 software at the MPW1PW91/3-21G level.<sup>26–29</sup> The fluorescence quantum yield was measured at 20 °C using quinine bisulfate in 1 M H<sub>2</sub>SO<sub>4</sub> ( $\phi_{fr}$  = 0.546) as the reference.<sup>30</sup>

### Synthesis and characterization of 4-MeB

The synthetic route to **4-MeB** is shown in Scheme 1. 5-Methoxy-2-(4-pyridyl)thiazole (**4-MPT**) was synthesized by following a previously reported method with minor modifications.<sup>19,25</sup>

**4-MeB** was obtained according to the procedure shown below. Ethyl bromoacetate (0.44 mL, 3.94 mmol) was added into a stirred solution of **4-MPT** (500 mg, 2.60 mmol) in dried chloroform (15 mL) at 20 °C under an argon atmosphere. After the mixture had been stirred for 12 h, the reaction solution was concentrated under reduced pressure. The residue was recrystallized from EtOAc, affording the final product (746 mg). Yield: 80%. ESI-MS:  $m/z$  = 279 [M + H – Br]; <sup>1</sup>H NMR (400 MHz, CD<sub>3</sub>CN, 25 °C, TMS):  $\delta$  = 1.30 (t, 3H), 4.11 (s, 3H), 4.29 (q,  $J$  = 7.12 Hz, 2H), 5.47 (s, 2H), 7.59 (s, 1H), 8.30 (d, 2H) and 8.73 (d, 2H); <sup>13</sup>C NMR (100 MHz, CD<sub>3</sub>CN):  $\delta$  = 13.2, 59.8, 62.6, 62.8, 121.7, 126.2, 145.8, 145.9, 148.8, 165.8 and 170.0. Elemental analysis: calc. for C<sub>13</sub>H<sub>15</sub>BrN<sub>2</sub>O<sub>3</sub>S: C, 43.46; H, 4.21; N, 7.80. Found: C, 42.74; H, 4.19; N, 7.66%.

## 3. Results and discussion

### The absorption spectrum of 4-MeB in different solvents

The absorption spectrum of **4-MeB** in different solvents is shown in Fig. 1. In the UV region of 300–400 nm, an absorption peak with a large molar absorption coefficient of about 10<sup>4</sup> M<sup>−1</sup> cm<sup>−1</sup> (Table 1) is observed that originates from a  $\pi \rightarrow \pi^*$  electronic transition. In addition, two absorption peaks with smaller molar absorption coefficients of about 10<sup>3</sup> M<sup>−1</sup> cm<sup>−1</sup> (Table 1) in the region between 450 and 600 nm emerge in the absorption spectrum of **4-MeB** in

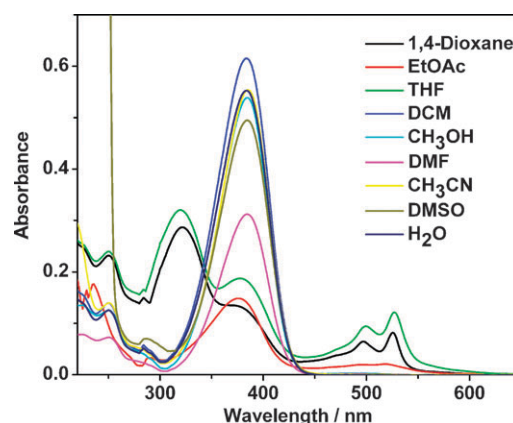


**Fig. 1** The absorption spectrum of **4-MeB** in different solvents ( $c = 2.5 \times 10^{-5}$  mol L<sup>−1</sup>).

**Table 1** Photophysical data of **4-MeB** in different solvents at room temperature

Medium	$\lambda_{\text{max}}^{\text{abs}}/\text{nm}$ (absorption coefficient/ 10 <sup>4</sup> M <sup>−1</sup> cm <sup>−1</sup> )	$\lambda_{\text{max}}^{\text{em}}/\text{nm}$ ( $\lambda_{\text{ex}} = 310$ nm)	$\lambda_{\text{max}}^{\text{em}}/\text{nm}$ ( $\lambda_{\text{ex}} = 366$ nm)	$\phi$
1,4-Dioxane	322 (1.14) 373 (0.54) 497 (0.26) 525 (0.32)	385	439	0.308
EtOAc	376 (0.60) 497 (0.078) 518 (0.083)	388	441	0.113
THF	320 (1.28) 377 (0.75) 499 (0.38) 527 (0.48)	388	453	0.330
DCM	394 (2.20)	437	441	0.366
CH <sub>3</sub> OH	385 (2.15)	417	454	0.033
DMF	383 (1.26)	397	448	0.377
CH <sub>3</sub> CN	385 (2.20)	417	456	0.035
DMSO	385 (1.98)	411	465	0.016
H <sub>2</sub> O	383 (2.20)	419	452	0.026

solvents with smaller  $\epsilon$  values, such as 1,4-dioxane, EtOAc and THF. With increasing  $\epsilon$  value, the absorbance in the visible region decreases, implying that the absorption of **4-MeB** in the visible region is highly sensitive to its surroundings. The changes in the absorption spectrum and color of **4-MeB** (Fig. 1 and Fig. 2) in different solvents suggest its potential as a probe for solvents. As revealed in Fig. 3 and Fig. S1 (see ESI<sup>†</sup>), in THF, EtOAc and 1,4-dioxane, the absorbance of **4-MeB** in the visible region displays a linear dependence on its concentration, indicating the absorption band is due to the molecular nature of **4-MeB**. Comparing with the absorption spectrum of **4-MPT** in all the employed

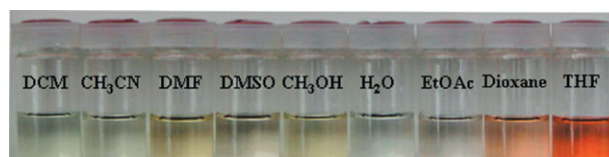


**Fig. 2** Color change of **4-MeB** in different solvents ( $c = 1.0 \times 10^{-4}$  mol L<sup>−1</sup>).

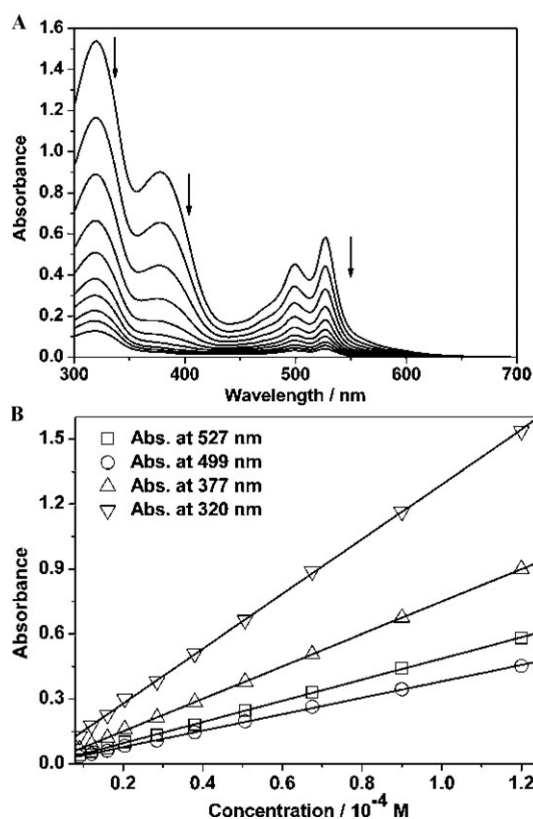


**Fig. 3** (A) Change in the absorption spectrum and (B) the absorbance change at a specific wavelength in THF with decreasing concentration for **4-MeB**. The solid lines in (B) represent fit lines of the absorbance at a specific wavelength to the concentration of **4-MeB**. The concentration range of **4-MeB** was from  $1.2 \times 10^{-4}$  to  $1.0 \times 10^{-5}$  mol L $^{-1}$ .

solvents, it is notable that a remarkable bathochromic shift of  $\lambda_{\text{max}}^{\text{abs}}$  in the UV region occurs in the absorption spectrum of **4-MeB**, similar to that of protonated **4-MPT** (**4-MPT-H $^{+}$** ) (Chart 1). This is ascribed to the similar bonding nature between the nitrogen atom in the pyridyl ring of **4-MPT** and the ethoxy carbonyl methyl group/proton.<sup>25</sup> Compared with that of **4-MePF** (Chart 1),<sup>19</sup> a blue-shift of  $\lambda_{\text{max}}^{\text{abs}}$  in the UV region and two absorption peaks in the visible region (**4-MeB** in solvents with smaller  $\epsilon$  values) were observed in the absorption spectrum of **4-MeB**, which is attributed to the different bonding characteristics between the pyridinium cation and corresponding anion parts of the two molecules. In **4-MeB**, the fourth bond to the nitrogen atom in the pyridyl

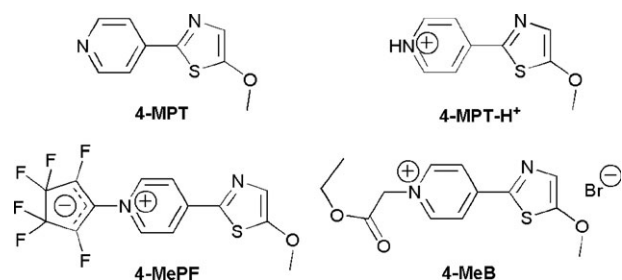


**Chart 1** The molecular structures of **4-MPT**, **4-MPT-H $^{+}$** , **4-MePF** and **4-MeB**.

ring is formed with a methylene group, and only one ionic bond exists between the pyridinium cation moiety and the bromide anion; while for **4-MePF**, a covalent bond conjugates the cation and anion moieties. Thus, from the absorption spectra of **4-MPT**, **4-MPT-H $^{+}$** , **4-MePF** and **4-MeB**, it is easy to conclude that different molecular structures determine their various photophysical properties, which may guide us to design functional compounds based on our demands of their photophysical properties.

The addition of  $\text{AgPF}_6$  into THF or 1,4-dioxane solutions of **4-MeB** made its absorption in the visible region disappear (Fig. 4 and Fig. S2 (see ESI $^{\dagger}$ )). When  $\text{AgPF}_6$  was added,  $\text{Ag(I)}$  reacted with bromide anion to produce an  $\text{AgBr}$  precipitate and resulted in the formation of **4-MeP** (Fig. 4B). Because of the high symmetry and small polarization potential of the  $\text{PF}_6^-$  anion, it is impossible for it to have a strong interaction with the 1-(ethoxy-carbonyl-methyl)-4-[2-(5-methoxy)-thiazolyl]-pyridinium cation (**4-Me $^{+}$** ). Thus, the **4-Me $^{+}$**  cation and  $\text{PF}_6^-$  anion exist as free ions. A subsequent addition of  $(n\text{-Bu})_4\text{NBr}$  to the above mixture recovered **4-MeB**, and thus restored the absorption of **4-MeB** in the visible region (Fig. 4). This regenerated spectral behaviour further confirms that the absorption of **4-MeB** in the visible region depends on an interaction between the bromide anion and pyridinium cation.

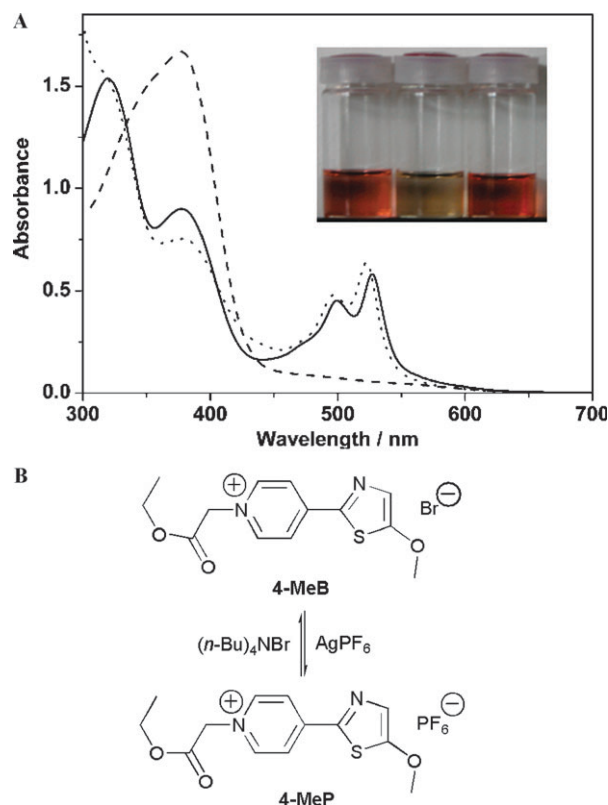


**Fig. 4** (A) Absorption spectra of **4-MeB** in THF ( $c = 1.20 \times 10^{-4}$  mol L $^{-1}$ ) (solid line: **4-MeB** only, dashed line: **4-MeB** with  $\text{AgPF}_6$  added, dotted line: **4-MeB** with  $\text{AgPF}_6$  and  $(n\text{-Bu})_4\text{NBr}$  added sequentially). Inset: the color change of **4-MeB** in THF (from left to right: **4-MeB** only, **4-MeB** with  $\text{AgPF}_6$  added, **4-MeB** with  $\text{AgPF}_6$  and  $(n\text{-Bu})_4\text{NBr}$  added sequentially). (B) The interconversion between **4-MeB** and **4-MeP**.



The addition of  $(n\text{-Bu})_4\text{NI}$  into the **4-MeP** solution also restored the absorption band in the visible region (Fig. S3, see ESI†), indicating that the **4-Me**<sup>+</sup> cation and iodide anion also form a tight ion pair. Because of the bigger ionic radius and polarization potential of iodide anions compared to bromide anions, the maximum absorption wavelength displayed a distinct red-shift. However, the addition of  $\text{Me}_4\text{NCl}$  to a solution of **4-MeP** brought no changes to the absorption spectrum of **4-MeP** (Fig. S4, see ESI†), because the smaller ionic radius and polarization potential of the chloride anion does not allow it to form a tight ion pair with the **4-Me**<sup>+</sup> cation. When a neutral electron donor,  $\text{Et}_3\text{N}$ , was added to a solution of **4-MeP**, no obvious changes were detected (Fig. S5, see ESI†), demonstrating that  $\text{Et}_3\text{N}$  shows no strong interactions with the  $\pi$  cation **4-Me**<sup>+</sup>, which can be attributed to their unmatched molecular orbitals.

### Theoretical calculations of **4-MeB** and the **4-Me**<sup>+</sup> cation

To further interpret the absorption properties of **4-MeB**, theoretical calculations were performed on this system, both for the entire neutral **4-MeB** molecule and the free cation **4-Me**<sup>+</sup>, at the MPW1PW91/3-21G level using GAUSSIAN 03.

For the free cation **4-Me**<sup>+</sup>, the highest occupied molecular orbital (HOMO) is mainly located on the methoxy-thiazolyl group and the lowest unoccupied molecular orbital (LUMO) on the pyridyl ring (Fig. 5). As shown in Table 2, the TD-DFT calculation results demonstrate that the absorption of the **4-Me**<sup>+</sup> cation mainly arises from HOMO to LUMO, HOMO – 3 to LUMO and HOMO – 1 to LUMO transitions. The calculated transitions are in good agreement with the absorption spectra of **4-MeB** in solvents with larger  $\epsilon$  values, e.g. water, in which one intense excitation at 367 nm is

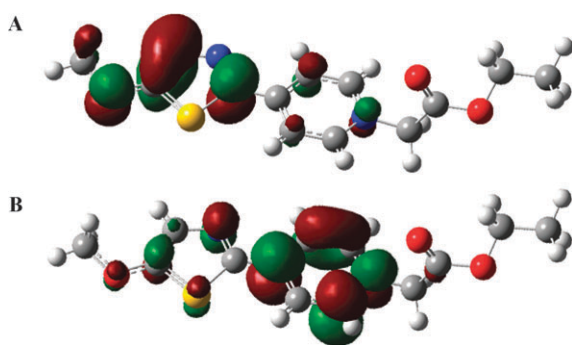


**Fig. 5** The (A) HOMO and (B) LUMO of the **4-Me**<sup>+</sup> cation calculated at the MPW1PW91/3-21G level using GAUSSIAN 03.

**Table 2** Excitations of the **4-Me**<sup>+</sup> cation that contribute to its transitions in 300–450 nm range, along with their relative contributions given by their expansion coefficient

$\lambda_{\text{ex}}/\text{nm}$	$E_{\text{ex}}/\text{eV}$	Oscillator strength ( $f$ )	Excited state	Expansion coefficient
367.33	3.3753	0.5133	HOMO $\rightarrow$ LUMO	0.64622
319.39	3.8819	0.0016	HOMO – 3 $\rightarrow$ LUMO	0.66366
309.86	4.0013	0.0050	HOMO – 1 $\rightarrow$ LUMO	0.68819

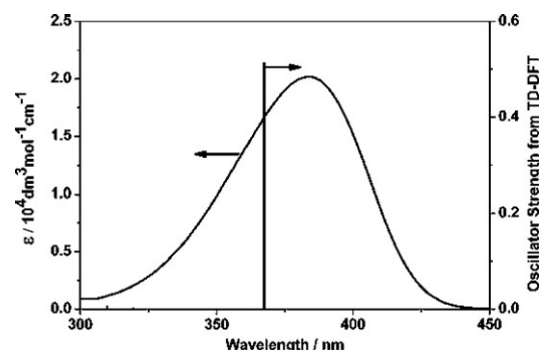


**Fig. 6** The absorption spectrum of **4-MeB** in water at r.t. and the calculated transition energies (from TD-DFT) of the **4-Me**<sup>+</sup> cation shown as bars.

observed, plus two weak excitations at 319 and 309 nm, with no excitations being found in the visible region (Fig. 6 and Table 2). Thus, in solvents with larger  $\epsilon$  values, **4-MeB** is ionized into free ions and there is no significant electronic coupling between the bromide anion and the **4-Me**<sup>+</sup> cation in the ground state.

As the absorption spectrum of **4-MeB** in the visible region depends on interactions between the bromide anion and pyridinium cation, different distances between the bromide anion and nitrogen atom of the pyridyl ring may result in the different absorption properties seen for **4-MeB**. To investigate the influence of this distance on the absorption properties of **4-MeB**, theoretical calculations were performed while changing it from 4.05 to 9.45 Å. This shows that the HOMO, LUMO, LUMO + 2 and LUMO + 3 of **4-MeB** hold their locations at the bromide anion, thiazolyl-pyridyl moiety and ethoxy carbonyl methyl group, respectively (Fig. 7A–D and Fig. S6–S9, see ESI†).

TD-DFT calculations on **4-MeB** with different distances between the bromide anion and nitrogen atom of the pyridyl ring were also executed. **4-MeB** with a distance of 4.05 Å between the bromide anion and nitrogen atom of the pyridyl ring is exemplified here to investigate the origin of the absorption properties of **4-MeB**. The calculation results are in good agreement with the absorption spectra of **4-MeB** in solvents with smaller  $\epsilon$  values, such as THF (Fig. 8 and Table 3). Besides the excited state at about 335 nm, two additional excited states at about 440 and 455 nm are also observed in the TD-DFT calculation results (Fig. 8). As demonstrated in Table 3, the excitations of **4-MeB** in the UV region mostly result from an electron transition from HOMO – 3 to LUMO, and those in the visible region mostly from HOMO to LUMO + 2 and HOMO to LUMO + 3, which implies that absorption in the visible region originates from bromide anion  $\rightarrow$  thiazolyl-pyridinium cation charge-transfer.

To further study the influence of the interaction between the bromide anion and the **4-Me**<sup>+</sup> cation on the absorption band in the visible region of **4-MeB**, the relationship between the oscillator strength ( $f$ ) of the excitation from HOMO to LUMO + 2 and the distance between the bromide anion and nitrogen atom in the pyridyl ring was also investigated. With this distance varying from 4.05 to 9.45 Å, the  $f$  value of the excitation from HOMO to LUMO + 2 decreased (Fig. 9),

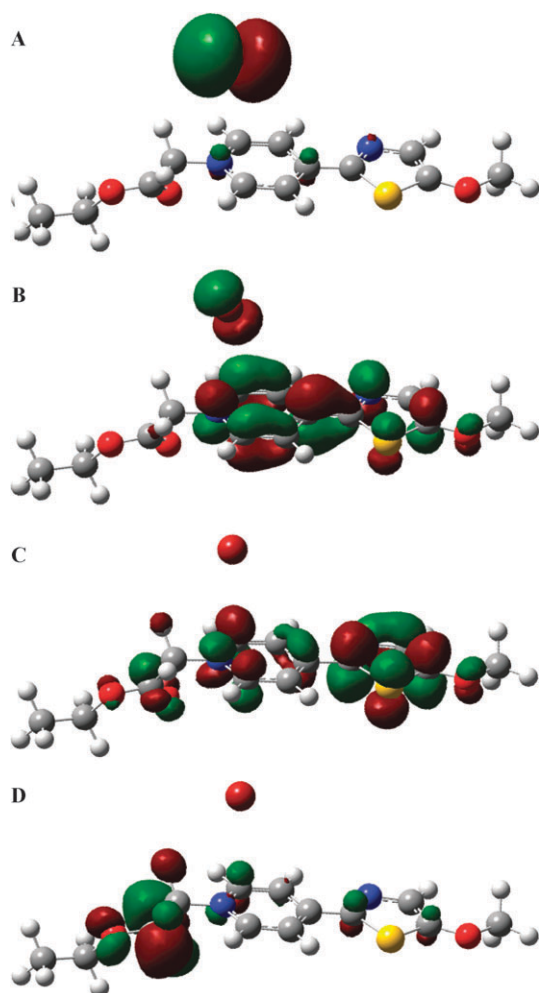


**Fig. 7** The (A) HOMO, (B) LUMO, (C) LUMO + 2 and (D) LUMO + 3 of **4-MeB** calculated at the MPW1PW91/3-21G level using GAUSSIAN 03 while the distance between the bromide anion and nitrogen atom of the pyridyl ring is set as 4.05 Å.

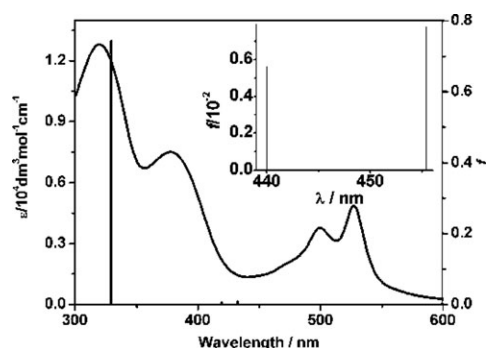


**Fig. 8** The absorption spectrum of **4-MeB** in THF at r.t. and the calculated transition energies (from TD-DFT) of **4-MeB** shown as bars. Inset: the magnified transition energies (from TD-DFT) of **4-MeB** in the visible region.

demonstrating that this excitation is tuned by the distance between the cation and the anion within the tight ion pair. Thus, it is concluded that only when the bromide anion and thiazolyl-pyridinium cation are strongly coupled in the ground state can absorption in the visible region be observed.

**Table 3** Excitations in **4-MeB** that contribute to its transitions in 300–600 nm range, along with their relative contributions given by their expansion coefficient

$\lambda_{\text{ex}}/\text{nm}$	$E_{\text{ex}}/\text{eV}$	Oscillator strength ( $f$ )	Excited state	Expansion coefficient
335.22	3.6986	0.7426	HOMO – 3 $\rightarrow$ LUMO + 1	0.60930
440.02	2.8177	0.0056	HOMO $\rightarrow$ LUMO + 3	0.51180
455.39	2.7226	0.0078	HOMO $\rightarrow$ LUMO + 2	0.68552

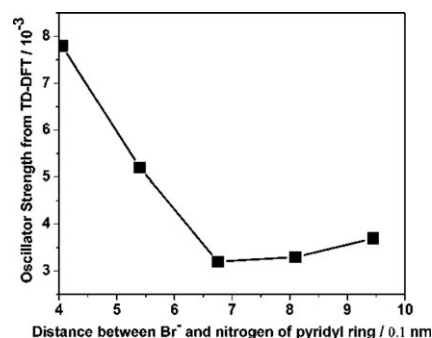


**Fig. 9** The dependence of the oscillator strength ( $f$ ) of the excitation from HOMO to LUMO + 2 on the distance between the bromide anion and the nitrogen atom in the pyridyl ring.

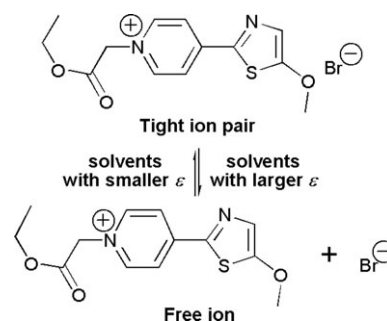


**Fig. 10** The interconversion of **4-MeB** in different solvents.

In association with the solvent-sensitive absorption spectra, the TD-DFT calculation results of the **4-Me<sup>+</sup>** cation and **4-MeB** confirm that **4-MeB** exists in different forms in different solvents. In solvents with larger  $\epsilon$  values, **4-MeB** is ionized into free ions and mainly exhibits electronic transition behavior of the **4-Me<sup>+</sup>** cation. In the solvents with smaller  $\epsilon$  values, **4-MeB** exists in the form of tight ion pair and exhibits not only the absorption properties of the **4-Me<sup>+</sup>** cation, but also those characteristic of **4-MeB** in the form of the tight ion pair. Fig. 10 describes the different forms of **4-MeB** in different solvents.

### The dual-emissive fluorescent property of **4-MeB**

Fig. 11 shows the emission/excitation spectra of **4-MeB** in acetonitrile at different excitation/emission wavelengths. Upon changing the excitation wavelength from 310 to 366 nm, a large bathochromic shift of the emission peak (from 417 to 456 nm) is observed in the emission spectrum of **4-MeB**. The

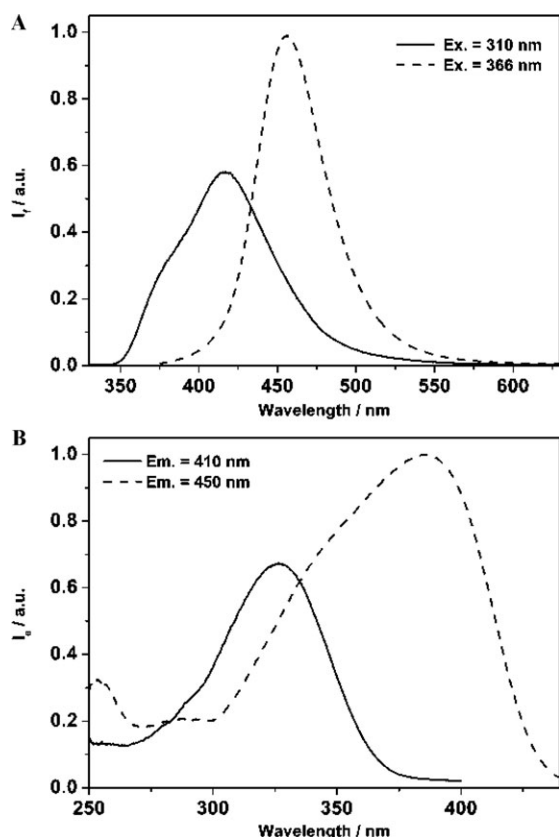


**Fig. 11** (A) Emission spectra of **4-MeB** in acetonitrile upon excitation at 310 and 366 nm. (B) Excitation spectra of **4-MeB** in acetonitrile at emission wavelengths of 410 and 450 nm.

excitation spectrum of **4-MeB** exhibits a distinct bathochromic trend, with the emission wavelength shifted from 410 to 450 nm. Similar results were also obtained with the other selected solvents (Fig. S10–S17, see ESI†) and Table 1). Considering together the emission/excitation spectra of **4-MeB** at different excitation/emission wavelengths in different solvents (Fig. 11 and Fig. S10–S17 (see ESI†)), it is easy to conclude that a shorter excitation wavelength benefits the higher energy emission and a longer excitation wavelength benefits the lower energy emission. In all of the selected solvents, the fluorescence decay curves were fitted to double-exponential decays (Fig. S18–S26, see ESI†), demonstrating that two fluorescence decay processes exist. Further studies on the lifetimes of **4-MeB** in all the adopted solvents demonstrate that the fraction of the longer lifetime component decreases, with the emission wavelength red-shifted at the same excitation wavelength (Tables S1–S9, see ESI†), except for the DMF solution of **4-MeB**. This suggests that shorter lifetimes correspond to the longer wavelength emissions.

## Conclusions

In summary, a new fluorophore, **4-MeB**, has been synthesized based on **4-MPT**, and its photophysical properties studied in detail. Investigations of its absorption spectra and theoretical calculation results demonstrate that the existence of different forms of **4-MeB** in different solvents determine its

solvent-sensitive absorption properties. In solvents with larger  $\epsilon$  values, **4-MeB** is ionized into free ions and shows a thiazolyl-pyridinium cation-centered  $\pi \rightarrow \pi^*$  electronic transition absorption band in the UV region. In solvents with smaller  $\epsilon$  values, such as THF, 1,4-dioxane and EtOAc, **4-MeB** exists in the form of a tight ion pair and displays a bromide anion-dependent absorption band in the visible region, except for that in the UV region. Studies on the effect of a neutral electron donor, Et<sub>3</sub>N, and other monovalent anions, such as PF<sub>6</sub><sup>−</sup>, I<sup>−</sup> and Cl<sup>−</sup>, on the absorption spectrum of the **4-Me**<sup>+</sup> cation illustrated that only I<sup>−</sup> displays a similar influence to that of the bromide anion. This is because of their suitable ionic radii and polarization potentials, further indicating that **4-MeB** exists in the form of a tight ion pair in solvents with smaller  $\epsilon$  values, and that its absorption behaviour depends on the bromide anion. With the help of theoretical calculations, the characteristic absorption in visible region can be attributed to charge-transfer from the bromide anion to the thiazolyl-pyridinium cation, and it can be tuned by the distance between the bromide anion and the nitrogen atom of the pyridyl ring. Studies on its fluorescence emission properties show that **4-MeB** exhibits a dual-emissive property in all the solvents we employed, and that the emission positions and relative intensities are influenced by the excitation wavelength.

## Acknowledgements

The authors thank the NSFC(20821091, 20771009 and 20731160001) and PKU for financial support.

## References

- Y. S. Rosokha, S. V. Lindeman, S. V. Rosokha and J. K. Kochi, *Angew. Chem., Int. Ed.*, 2004, **43**, 4650.
- P. A. Gale, L. J. Twyman, C. I. Handlin and J. L. Sessler, *Chem. Commun.*, 1999, 1851.
- C. B. Black, B. Andrioletti, A. C. Try, C. Ruiperez and J. L. Sessler, *J. Am. Chem. Soc.*, 1999, **121**, 10438.
- E. Corradi, S. V. Meille, M. T. Messina, P. Metrangolo and G. Resnati, *Angew. Chem., Int. Ed.*, 2000, **39**, 1782.
- S. V. Lindeman, J. Hecht and J. K. Kochi, *J. Am. Chem. Soc.*, 2003, **125**, 11597.
- B. L. Schottel, H. T. Chifotides, M. Shatruck, A. Chouai, L. M. Pérez, J. Bacsá and K. R. Dunbar, *J. Am. Chem. Soc.*, 2006, **128**, 5895.
- A. Perez-Velasco, V. Gortea and S. Matile, *Angew. Chem., Int. Ed.*, 2008, **47**, 921.
- A. Wada, M. Watanabe, Y. Yamanoi and H. Nishihara, *Chem. Commun.*, 2008, 1671.
- P. D. Beer and P. A. Gale, *Angew. Chem., Int. Ed.*, 2001, **40**, 486.
- Supramolecular Chemistry of Anions*, ed. A. Bianchi, K. Bowman-James and E. Garcia-España, Wiley-VCH, New York, 1997.
- G. R. Desiraju and T. Steiner, *The Weak Hydrogen Bond in Structural Chemistry and Biology*, Oxford University Press, Oxford, 1999.
- M. M. G. Antonisse and D. N. Reinhoudt, *Chem. Commun.*, 1998, 443 and refs. 8–21 therein.
- J. S. Kim and D. T. Quang, *Chem. Rev.*, 2007, **107**, 3780.
- D. R. Turner, M. J. Paterson and J. W. Steed, *Chem. Commun.*, 2008, 1395.
- Y. Li and A. H. Flood, *Angew. Chem., Int. Ed.*, 2008, **47**, 2649.
- F. P. Schmidtchen and M. Berger, *Chem. Rev.*, 1997, **97**, 1609.
- H. Lee, M. Diaz, C. B. Knobler and M. F. Hawthorne, *Angew. Chem., Int. Ed.*, 2000, **39**, 776 and references therein.
- M. Mascari, A. Armstrong and M. D. Bartberger, *J. Am. Chem. Soc.*, 2002, **124**, 6274.

- 19 Z.-X. Li, W. Sun, Y.-F. Yue, M.-H. Zheng, C.-H. Xu, J.-Y. Jin, C.-J. Fang and C.-H. Yan, *Tetrahedron Lett.*, 2007, **48**, 7675.
- 20 E. M. Kosower, *J. Am. Chem. Soc.*, 1958, **80**, 3253; E. M. Kosower, *J. Am. Chem. Soc.*, 1958, **80**, 3261; E. M. Kosower, *J. Am. Chem. Soc.*, 1958, **80**, 3267; E. M. Kosower, J. A. Skorcz, W. M. Schwarz and J. W. Patton, *J. Am. Chem. Soc.*, 1960, **82**, 2188.
- 21 E. M. Kosower and M. Mohammad, *J. Am. Chem. Soc.*, 1968, **90**, 3271.
- 22 J. W. Larsen, A. G. Edwards and P. Dobi, *J. Am. Chem. Soc.*, 1980, **102**, 6780.
- 23 A. M. Moran, S. Park and N. F. Scherer, *J. Phys. Chem. B*, 2006, **110**, 19771.
- 24 J. H. Fendler and L.-J. Liu, *J. Am. Chem. Soc.*, 1975, **97**, 999.
- 25 M.-H. Zheng, J.-Y. Jin, W. Sun and C.-H. Yan, *New J. Chem.*, 2006, **30**, 1192.
- 26 M. J. Frisch, G. W. Trucks, H. B. Schlegel, G. E. Scuseria, M. A. Robb, J. R. Cheeseman, J. A. Montgomery, Jr, T. Vreven, K. N. Kudin, J. C. Burant, J. M. Millam, S. S. Iyengar, J. Tomasi, V. Barone, B. Mennucci, M. Cossi, G. Scalmani, N. Rega, G. A. Petersson, H. Nakatsuji, M. Hada, M. Ehara, K. Toyota, R. Fukuda, J. Hasegawa, M. Ishida, T. Nakajima, Y. Honda, O. Kitao, H. Nakai, M. Klene, X. Li, J. E. Knox, H. P. Hratchian, J. B. Cross, V. Bakken, C. Adamo, J. Jaramillo, R. Gomperts, R. E. Stratmann, O. Yazyev, A. J. Austin, R. Cammi, C. Pomelli, J. Ochterski, P. Y. Ayala, K. Morokuma, G. A. Voth, P. Salvador, J. J. Dannenberg, V. G. Zakrzewski, S. Dapprich, A. D. Daniels, M. C. Strain, O. Farkas, D. K. Malick, A. D. Rabuck, K. J. Raghavachari, B. Foresman, J. V. Ortiz, Q. Cui, A. G. Baboul, S. Clifford, J. Cioslowski, B. B. Stefanov, G. Liu, A. Liashenko, P. Piskorz, I. Komaromi, R. L. Martin, D. J. Fox, T. Keith, M. A. Al-Laham, C. Y. Peng, A. Nanayakkara, M. Challacombe, P. M. W. Gill, B. G. Johnson, W. Chen, M. W. Wong, C. Gonzalez and J. A. Pople, *GAUSSIAN 03 (Revision B.05)*, Gaussian Inc., Pittsburgh, PA, 2003.
- 27 P. J. Hay and W. R. Wadt, *J. Chem. Phys.*, 1985, **82**, 270; P. J. Hay and W. R. Wadt, *J. Chem. Phys.*, 1985, **82**, 299.
- 28 W. R. Wadt and P. J. Hay, *J. Chem. Phys.*, 1985, **82**, 284.
- 29 C. Lee, W. Yang and R. G. Parr, *Phys. Rev. B: Condens. Matter Mater. Phys.*, 1988, **37**, 785.
- 30 J. N. Demas and G. A. Grosby, *J. Phys. Chem.*, 1971, **75**, 991.